



Metamaterial Beam with Bistable and Monostable-Hardening Attachments for Broad-Band Vibration Attenuation and Energy Harvesting

Che Xu  and Liya Zhao  

School of Mechanical and Manufacturing Engineering, University of New South Wales, Sydney, NSW 2052, Australia

liya.zhao2@unsw.edu.au

Abstract. Dynamic local resonating (LR) metastructures possess the ability to suppress the propagation of vibrations within a specific frequency range known as a bandgap. However, metastructures with pure linear local resonators have limited bandgap size and inevitably form new resonating peaks close to the bandgap. This paper proposes a metastructure that features alternatively arranged oscillators with bistable and monostable cubic hardening nonlinearities, as well as electromechanical coupling. This design effectively suppresses high-amplitude resonating transmission peaks near the bandgap and maintains the bandgap at high excitation levels. In addition, it can create a broad bandwidth with high power output, which can be applied as a practical source of electrical energy, thereby forming a well-balanced and performance-enhanced dual-functional metastructure for vibration suppression and energy harvesting. The proposed metastructure is established and calculated using a distributed-parameter model. The influence of nonlinearity stiffness and electrical-mechanical coupling index are investigated. Results show that enhanced performance of both vibration attenuation and energy harvesting can be realized with the proposed metastructure at a large range of excitation level. The parametric results offer a valuable reference for the development of dual-functional metastructures for simultaneous vibration suppression and energy harvesting.

Keywords: Metastructure · Vibration suppression · Energy harvesting

1 Introduction

Dynamic locally resonant (LR) metastructures are finite structures inspired by phononic metamaterials that are assembled with periodically arranged local resonators on a host structure. These metastructures can attenuate vibration from propagating within a specific frequency range, which is known as a bandgap [1, 2]. These local resonators allow for a discrete distribution of mass and can be integrated into the host structure during the fabrication state [3], reducing the cost of assemble and maintenance, therefore can

be considered as an ideal replacement for the traditional low-degree-of-freedom vibration attenuation systems to suppress the vibration of a host structure at low frequencies. However, in traditional metastructures, the bandgaps are quite narrow, and new resonating peaks close to the bandgap can be inevitably formed after integrating the local resonators on a host structure, endangering the host structure if the external excitations are around these frequencies. Therefore, there has been increasing research on performance enhancement of vibration suppressions in metastructures. Feasible solutions including frequency tuning [4–6], utilizing specific natural frequency patterns for local resonators [7–9], applying structural nonlinearities, etc. The studies that take the effect of nonlinearities for vibration attenuation involve applying monostable [10], bistable [11, 12], or piecewise nonlinearities [13] in metastructures. Separately, there is growing interest in converting the absorbed kinetic energy in the local resonators into electricity by incorporating transducers and energy harvesting circuits in these resonators. The transducer and the circuit serve as the energy conversion system as well as an extra electrical damping component to modify the attenuation performance of the metastructure [2]. However, for linear metastructures, the high-power-output bandwidth is narrow. The enhancement of dual functionality of energy harvesting and vibration attenuation with metastructures has received increasing attention only in recent years [7, 14–21]. To achieve a broad high-power-output bandwidth for vibrational energy harvesting, strong nonlinearity and high excitation levels across a wide range of vibration frequencies is usually required [22–25], however, introducing nonlinearity in metastructures often narrows or eliminates the effective bandgap for vibration attenuation, resulting in amplified vibrations instead of mitigation within the desired frequency range [12]. To address this challenge, there is a strong need to develop a novel design that provides a well-balanced performance of vibration suppression and energy harvesting across a large range of excitation levels as well as frequency range. This paper proposes a metastructure that features alternately arranged oscillators with bistable and monostable hardening nonlinearities, as well as electro-mechanical coupling. This design can effectively suppress the high-amplitude resonating transmission peaks near the bandgap in conventional metastructures and maintain the bandgap at a wide range of excitation levels. The proposed structure can also create a broader power bandwidth, thereby forming a well-balanced and performance-enhanced dual-functional metastructure for vibration suppression and energy harvesting. The proposed metastructure is established and calculated with a distributed model, which is validated through experiments. The influence of nonlinearity stiffness and electrical-mechanical coupling index are investigated.

2 Proposed Metastructure with Alternately Arranged Bistable and Monostable Hardening Oscillators

The schematic of the proposed metastructure is shown in Fig. 1. A host cantilever beam is subjected to base excitation displacement $w_b(t) = f \cos(\Omega_b t)$ at the fixed end ($p = 0$), with the amplitude of f and the frequency at Ω_b ; L is the length of the host beam. Several local resonating oscillators are attached and evenly positioned on the host cantilever to serve as vibration absorbers and energy harvesters. The oscillator closest to the fixed end of the beam is defined as the 1st local resonator, while the oscillator at the free

end is referred to as the S^{th} local resonator. p_j is the position coordinate of the j th oscillator, and q_j is the relative displacement of the local resonator with respect to the host beam. The oscillators are connected to the host beam via a nonlinear spring, with associated mechanical damping and electro-mechanical coupling. m_j and c_j are the equivalent lumped mass and damping of the j th local resonator, respectively. Two kinds of nonlinear oscillators, namely bistable oscillators and monostable hardening oscillators are applied and alternately arranged. $k_{1,j}$ and $k_{3,j}$ are the equivalent linear and cubic stiffness of the j th resonator, respectively. In bistable oscillators $k_{1,j}$ is negative, while for monostable oscillators $k_{1,j}$ is positive. $k_{3,j}$ is positive for all oscillators. θ_j , $C_{p,j}$ are the electromechanical coupling constant and capacitance of the piezoelectric transducer on the j th oscillator, respectively.

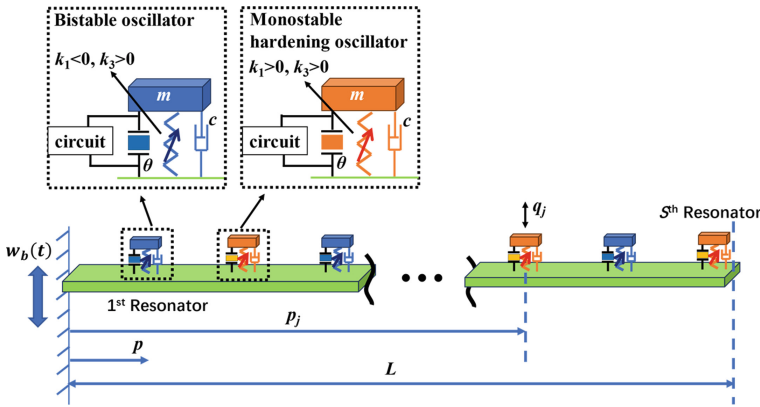


Fig. 1. Schematic of the proposed dual-functional nonlinear metastructure

The proposed nonlinear metastructure can then be modelled using a distributed-parameter electromechanically coupled model. The governing equations of the proposed metastructure can be expressed as

$$EI \frac{\partial^4 w_{rel}(p, t)}{\partial p^4} + c_s I \frac{\partial^5 w_{rel}(p, t)}{\partial p^4 \partial t} + c_a \frac{\partial w_{rel}(p, t)}{\partial t} + m \frac{\partial^2 w_{rel}(p, t)}{\partial t^2} - \sum_{j=1}^S \left(k_{1,j} q_j + k_{3,j} q_j^3 + c_j \frac{dq_j}{dt} + \theta_j v_j \right) \quad (1)$$

$$\delta(p - p_j) = -m \frac{d^2 w_b(t)}{dt^2} m_j \frac{d^2 q_j}{dt^2} + c_j \frac{dq_j}{dt} + k_{1,j} q_j + k_{3,j} q_j^3 + \theta_j v_j = -m_j \left(\frac{\partial^2 w_{rel}(p_j, t)}{\partial t^2} + \frac{d^2 w_b(t)}{dt^2} \right) + F_{m,j} \quad (2)$$

$$C_{p,j} \frac{dv_j}{dt} + \frac{v_j}{R_{L,j}} - \theta_j \frac{dq_j}{dt} = 0 \quad (3)$$

where the subscript j denotes the j th local resonator. $w_{rel}(p, t)$ is the relative displacement of the primary beam with respect to the base at the position coordinate p ; E is the Young's

modulus of the primary beam; I is the moment of inertia of the cross-section with respect to the neutral axis of the primary beam; c_s and c_a are the coefficients of strain rate damping and viscous damping, respectively; m is the mass density of the primary beam; $\delta(p)$ is the Dirac delta function; v_j is the voltage output of the piezoelectric transducer on the j th oscillator. Applying the expansion theorem, the relative displacement $w_{rel}(p, t)$ can be expressed as

$$w_{rel}(p, t) = \sum_{r=1}^N \phi_r(p) \eta_r(t) \quad (4)$$

where $\phi_r(p)$ is the r th eigenfunction of the host beam, and $\eta_r(t)$ is the modal coordinate of the r th mode. Inserting Eq. (4) into Eq. (1), multiplying the new equation with $\phi_s(p)$ and integrating it from $p = 0$ to L , then applying the mass-orthogonality condition for the eigenfunctions, the governing equation for the host beam can be expressed as:

$$\begin{aligned} \ddot{\eta}_r + 2\zeta_r \omega_r \dot{\eta}_r + \omega_r^2 \eta_r - \sum_{j=1}^S \left(k_{1,j} q_j + k_{3,j} q_j^3 + c_j \dot{q}_j + \theta_j v_j \right) \phi_r(p_j) \\ = - \int_0^L \phi_r(p) m \ddot{w}_b dp, \quad r = 1, 2, \dots, N \end{aligned} \quad (5)$$

where ζ_r is the damping factor of the r th mode of the host beam. The overdot denotes the derivative with respect to time t . Substituting Eq. (4) into Eq. (2), the governing equation for the i th local resonator can be expressed as

$$\begin{aligned} m_j \ddot{q}_j + c_j \dot{q}_j + k_{1,j} q_j + k_{3,j} q_j^3 + \theta_j v_j \\ = -m_j \sum_{r=1}^N \phi_r(p_j) \ddot{\eta}_r - m_j \ddot{w}_b \end{aligned} \quad (6)$$

Equations (3), (5) and (6) can then be rewritten in state-space form and numerically calculated in MATLAB. The mechanical parameters of the host beam and the oscillators, and the electro-mechanical coupling parameters in the following calculations are listed in Table 1.

The transmittance is defined as the ratio of root mean square (RMS) of the absolute displacement amplitude at the free end of the host beam to the RMS excitation amplitude at the fixed end, which is expressed as

$$T_r = \frac{(w_{rel}(L, t) + w_b(t))_{RMS}}{(w_b(t))_{RMS}} \quad (7)$$

The frequency range with $T_r < 1$ around the linear natural frequencies of the local resonators is referred to as the bandgap of transmission. The natural frequency of the host structure is around 11.5 Hz, which is the 2nd mode of the host structure. Figure 2(a) shows the performance of vibration attenuation, where the bistable and monostable cubic-hardening oscillators are alternately arranged and integrated with electro-mechanical coupling, and the linearized natural frequencies (intra-well resonant frequencies in the bistable case) are uniformly tuned to 11.3 Hz. For comparison, the results for the uniform linear metastructure, and the nonlinear metastructures with all-bistable configuration (i.e. all the local oscillators are the bistable oscillators with electro-mechanical coupling, with parameters for the 1st local resonator from the proposed metastructure in Table 1) and all-monostable configuration (with parameters for the 2nd local resonator in Table 1)

Table 1. System parameters

Parameters of the host beam	
Density, ρ	6000 kg/m ³
Beam Length, L	0.88 m
Beam Width, b	30×10^{-3} m
Beam Thickness, h	2.6×10^{-3} m
Modal damping ratios ζ_r ($r = 1 \sim 3$)	0.02, 0.02, 0.02
Young's modulus	69 GPa
Number of modes in expansion	3
Parameters of the local oscillators	
Equivalent Mass m_j	10.1×10^{-3} kg
Resonator damping c_j	0.03 Ns/m
Equivalent linear stiffness $k_{1,j}$ ($j = 1 \sim 8$)	Uniform: [-25.40 50.80 -25.40 50.80 -25.40 50.80 -25.40 50.80] N/m
	Graded: [-19.89 45.55 -25.85 58.24 -32.59 72.50 -40.11 88.32] N/m
Number of attachments	8
Cubic stiffness, $k_{3,j}$ ($j = 1 \sim 8$)	Uniform: [0.51 0.51 0.51 0.51 0.51 0.51 0.51 0.51] $\times 10^5$ N/m ³
	Graded: [0.40 0.40 0.40 0.40 0.40 0.40 0.40 0.40] $\times 10^5$ N/m ³
Electro-mechanical coupling parameters	
Capacitance, $C_{p,j}$	21.5 nF
Load resistance, $R_{L,j}$	500×10^3 Ω
electromechanical coupling constant, θ_j	4.4×10^{-4} N/V

are also included. The shaded area is the transmission bandgap for an undamped linear metastructure that is infinitely long, the left and right edges are given by $[\Omega_j, \Omega_j\sqrt{1 + \mu}]$ [2, 26], and Ω_j is equal to 11.3 Hz, which is the linearized natural frequency of all the resonators. The mass of the total mass of the local resonators to the host beam is $\mu = 0.196$. With the linearized natural frequency of the local resonators to be around 11.3 Hz, in Fig. 2(a), the bandgap is from 10.4 Hz to 12.8 Hz for the uniform linear metastructure. At such an excitation level, it found that the attenuation bandgap is narrowed to only 0.1 Hz (10.9 Hz to 11 Hz) for the metastructure with all-bistable configuration due to the extensive range of frequency with constant inter-well chaotic vibrations in the local oscillators. The width of the bandgap is maintained for the metastructure with the all-monostable configuration. However, in the all-monostable configuration, a resonance peak with the transmittance even higher than the all-linear case is induced, adversely adding potential risks of destruction to the host structure.

As to the proposed metastructure with alternate configuration, the resonance peak outside the bandgap at around 9 Hz is successfully attenuated, while the bandgap is maintained from 10.7 Hz to 13.6 Hz, forming a whole frequency range with low transmissibility. In terms of the power generation performance (see Fig. 2(b)), above a threshold of 200 mW, the bandwidth of metastructure with alternate oscillators is the broadest (ranging from 8.1 Hz to 10.3 Hz), which is 120% and 214% wider than the all-monostable and all-bistable configurations, respectively. Results show that the proposed metastructure with alternately arranged monostable hardening and bistable oscillators is advantageous among all the nonlinear metastructures for dual capabilities of vibration suppression and energy harvesting.

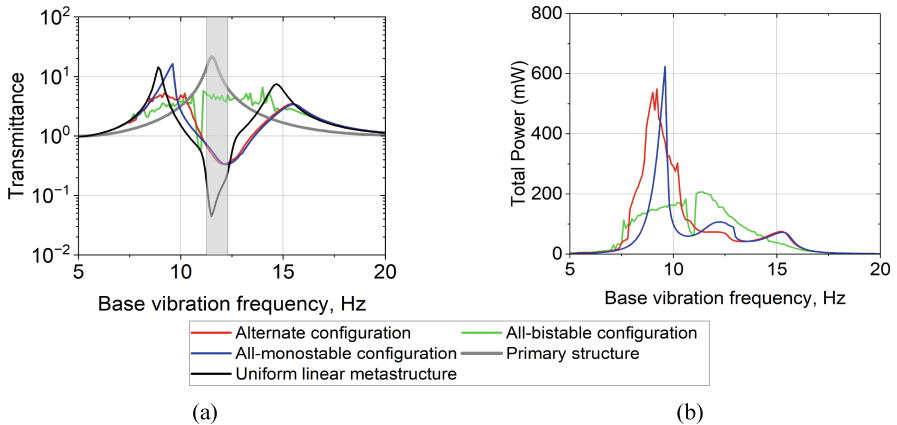


Fig. 2. Comparison of (a) transmittance and (b) total power at 9 m/s^2 for metastructures with alternate nonlinear oscillators, all-bistable oscillators and all-monostable oscillators.

Figure 3(a) shows the performance of vibration attenuation of the proposed uniform nonlinear metastructure with increased base acceleration. As the acceleration level increased, the transmittance gradually decreased around 9 Hz–10 Hz, showing that the resonance peak attenuation performance gets enhanced with elevated excitation levels. To have a deeper understanding, the time-domain responses are given in Figs. 4–5. At 9.6 Hz, as shown in Fig. 4, bistable oscillators are attached to the host beam when $j = 1, 3, 5$ and 7. Under $A_{\text{RMS}} = 1 \text{ m/s}^2$ (Fig. 4(a)), the bistable oscillators are vibrating as intra-well oscillations. As the A_{RMS} is increased to 5 m/s^2 (Fig. 4(b)), oscillators at $j = 3, 5$ and 7 start to vibrate as inter-well chaotic oscillations, however, the transmittance is much lower than the highest resonating transmittance in the uniform linear metastructure. As the A_{RMS} is increased to 9 m/s^2 (Fig. 4(c)), more bistable oscillators start to vibration as inter-well chaotic oscillations. Inter-well motions become more frequent, leading to an increased occurrence of out-of-phase motions between the primary structure and the oscillators, which causes a decrease of transmittance. Within the bandgap, e.g. under a base vibration frequency of 12.5 Hz, as shown in Fig. 5, all the oscillators vibration out-of-phase with the primary structure, inducing a low transmissibility. As shown in Fig. 4(c), a broad power bandwidth can be formed with the proposed metastructure, and the bandwidth is broadened with an increased excitation level.

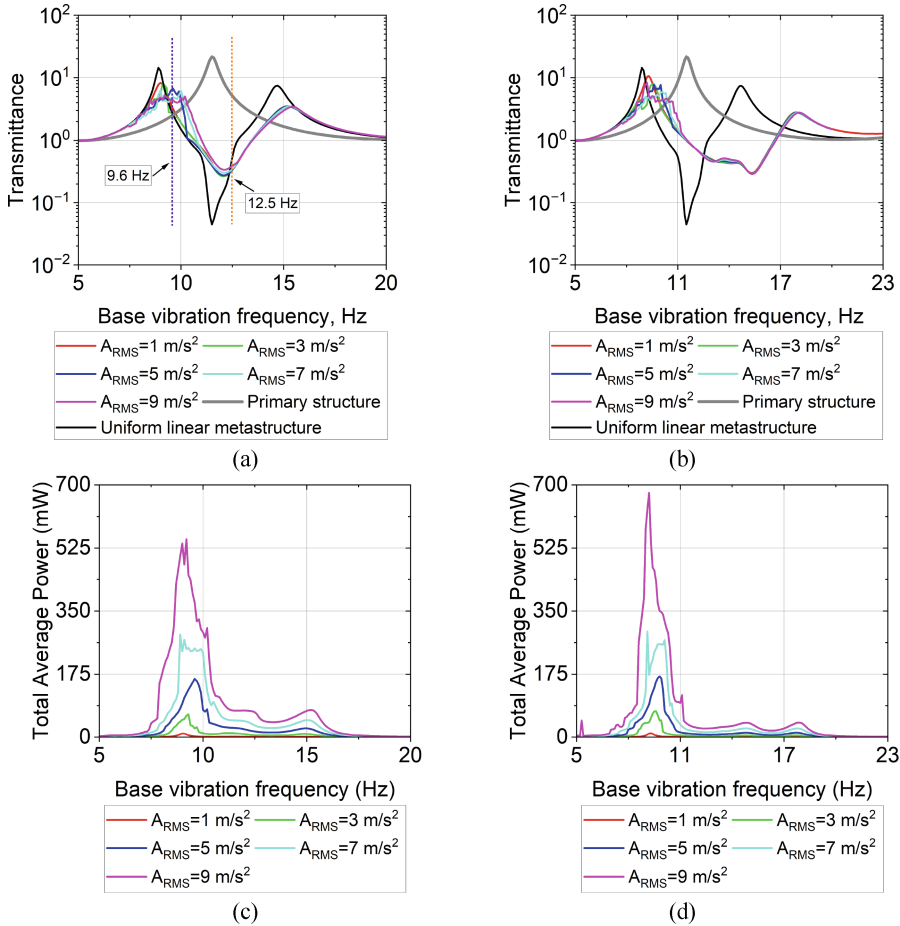


Fig. 3. Transmittance (upper row) and total power (lower row) of the (a)(c) uniform and (b)(d) graded nonlinear metastructure with alternate configuration under increased base acceleration from 1 m/s^2 to 9 m/s^2 .

The proposed metastructure has also been applied to a metastructure with a series of oscillators that have natural frequencies subjected to an increasing pattern (referred to as graded metastructure in the following). In this way, the out-of-phase oscillation between the oscillators and the host structure can be achieved within a broader range of frequencies, achieving a wider transmission bandgap. The proposed nonlinear metastructure with alternate nonlinear oscillators and linearized natural frequencies of [10 10.7 11.4 12.1 12.8 13.5 14.2 14.9] Hz has been calculated. As shown in Fig. 4(b) and Fig. 4(d), compared to the metastructure with uniform configuration (local resonators with identical linearized natural frequency), similar performances can be achieved with attenuated resonate peaks, maintained bandgap and wide power bandwidths, showing the universal effectiveness of the proposed nonlinear configuration on metastructures.

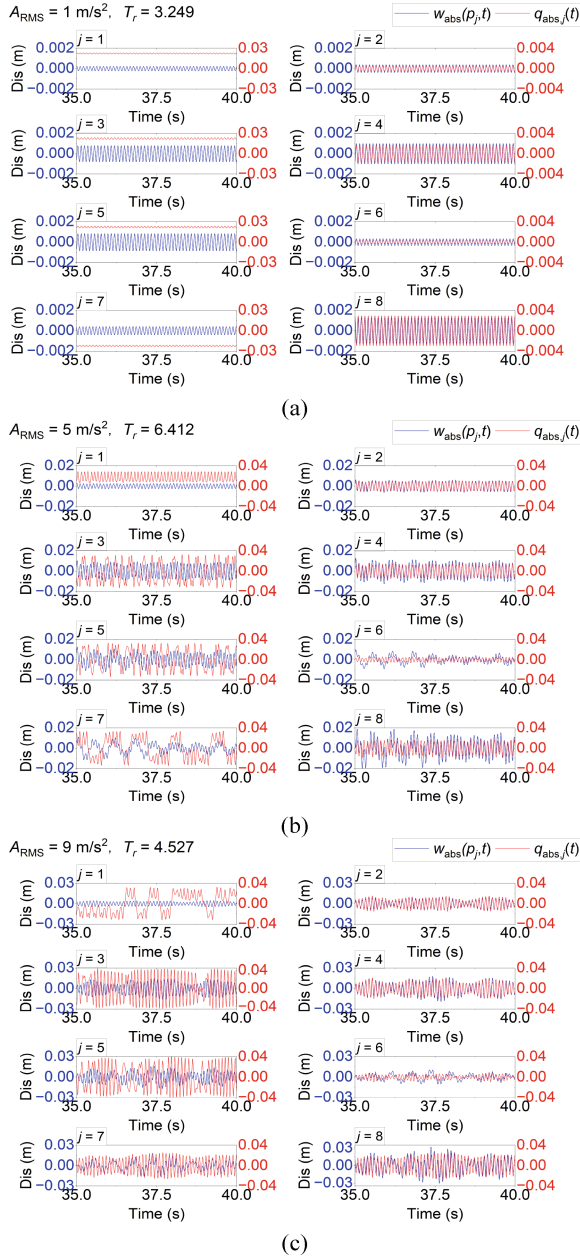


Fig. 4. Numerical time domain response of the primary structure (blue) and the local resonator (red) of each cell at 9.6 Hz under (a) $A_{\text{RMS}} = 1 \text{ m/s}^2$, (b) $A_{\text{RMS}} = 5 \text{ m/s}^2$ and (c) $A_{\text{RMS}} = 9 \text{ m/s}^2$,

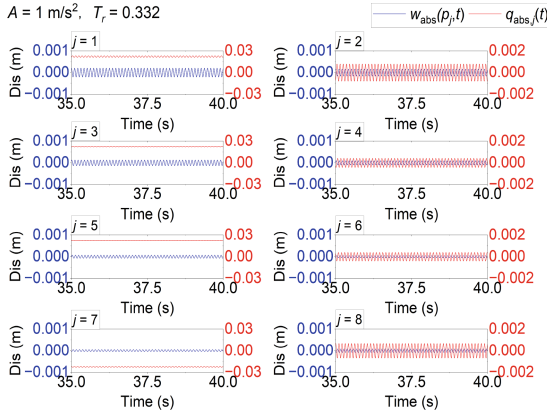


Fig. 5. Numerical time domain response of the primary structure (blue) and the local resonator (red) of each cell at 12.5 Hz under $A_{\text{rms}} = 1 \text{ m/s}^2$

3 Effect of Load Resistance and Electromechanical Coupling

A further investigation into the influence of load resistance on the performance of vibration suppression and energy harvesting is presented in Fig. 6–8. The parameter ke^2/ζ is applied to indicate the strength of the electro-mechanical coupling, where ke is the dimensionless electro-mechanical coupling coefficient calculated by $ke^2 = \theta_j^2 / (m_j \Omega_j^2 C_{p,j})$, and ζ is the damping ratio of the resonators calculated as $\zeta = c_j / (2m_j \Omega_j)$. The influence of R_L under a weak electro-mechanical coupling of $ke^2/\zeta = 8.455$ is given in Fig. 6. The transmittance result for a strong electro-mechanical coupling of $ke^2/\zeta = 33.820$ is given in Fig. 7. As shown in Fig. 6, under the weak coupling condition, the vibration suppression effect is not obviously affected under small or medium acceleration levels. However, under high acceleration levels (as shown in Fig. 6(c)) with excessively small or large load resistances, due to the reduced backward electrical damping, the transmittance around the resonating peaks becomes higher, suggesting that the resonance peak suppression capability is weakened. In the meantime, as shown in Fig. 7, it appears to have an optimal load resistance around $R_L = 100 \times 10^3 \Omega$ that induces the best performance for resonance peak attenuation and wide bandgap for all acceleration levels. To sum up, in order to achieve a better performance of vibration suppression, it is flexible for tuning the load resistance in weak electro-mechanical coupling, while careful adjustment of R_L is required to obtain the best performance in strong coupling conditions.

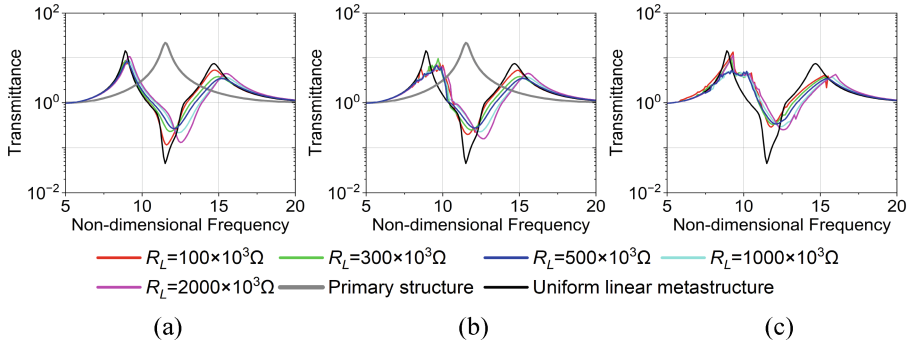


Fig. 6. Comparison of theoretical transmittance responses with different load resistances R_L , with weak coupling at $ke^2/\zeta = 8.455$ for the proposed nonlinear metastructure under (a) 1 m/s^2 , (b) 5 m/s^2 and (c) 9 m/s^2 .

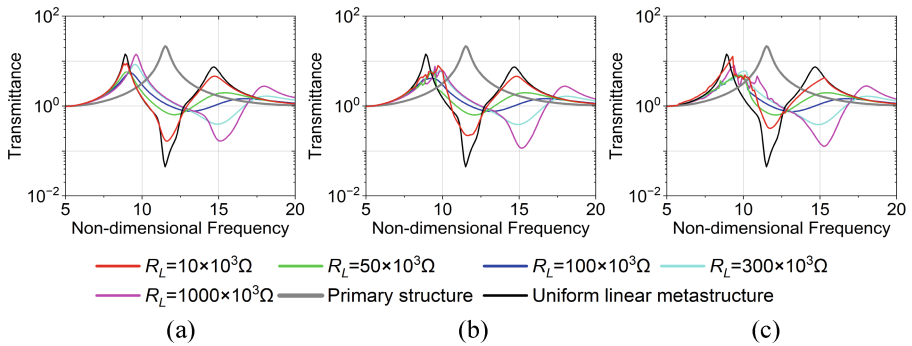


Fig. 7. Comparison of theoretical transmittance responses with different load resistances R_L , with strong coupling at $ke^2/\zeta = 33.820$ for the proposed nonlinear metastructure under (a) 1 m/s^2 , (b) 5 m/s^2 and (c) 9 m/s^2 .

The results of the power output for the uniform metastructure under weak and strong electro-mechanical coupling conditions with the variation of load resistances are given in Fig. 8 to assess the performance of the power output of the proposed metastructure. At the weak coupling condition (as shown in Fig. 8(a–c)), there appears to have an optimal load resistance (around $1000 \times 10^3 \Omega$) that leads to the highest output and bandwidth for high power output. Therefore, it is appropriate to use an identical optimal R_{Lopt} at all acceleration levels. In terms of strong coupling, as shown in Fig. 8(d), a double peak phenomenon at $R_L = 50 \times 10^3 \Omega$ and $300 \times 10^3 \Omega$ can be observed, which is a typical phenomenon of energy harvesting in strong electro-mechanical coupling conditions. At higher accelerations, the peak power and widest bandwidth are formed under different load resistances. To sum up, an optimal load resistance is recommended to obtain a higher power output and broader bandwidth of power in weak coupling conditions, while it is required to carefully adjust the load resistance over a range of load resistance to acquire a better performance of energy harvesting at different acceleration levels.

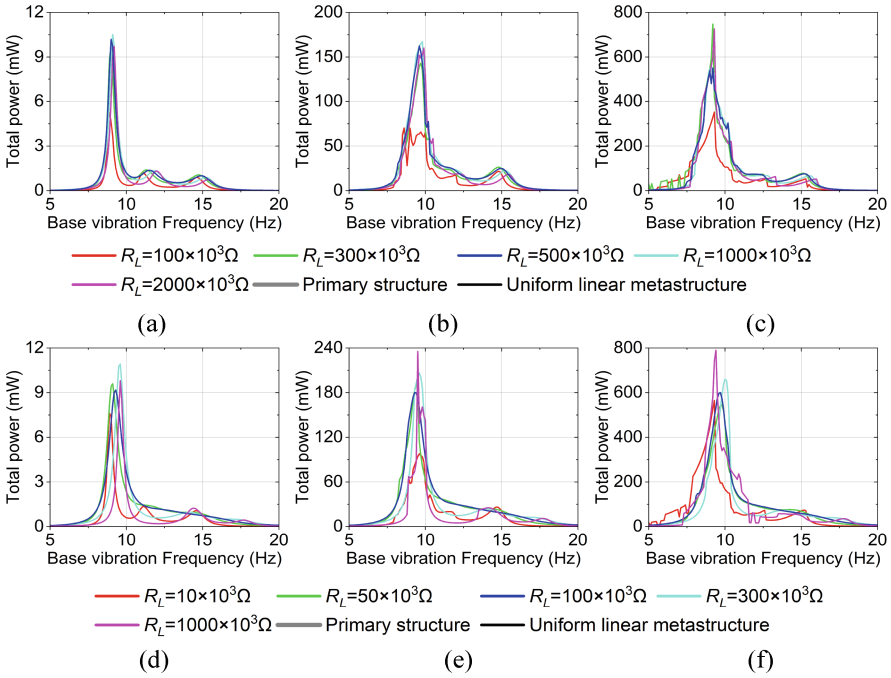


Fig. 8. Comparison of power output with different load resistances and electro-mechanical coupling of the proposed nonlinear metastructure: (a-c) $ke^2/\zeta = 8.455$; (d-f) $ke^2/\zeta = 33.820$. $A_{RMS} =$ (a)(d) 1 m/s^2 , (b)(e) 5 m/s^2 and (c)(f) 9 m/s^2 .

4 Conclusion

In this work, the performance of a novel nonlinear metastructure for simultaneous vibration suppression and energy harvesting has been investigated. The proposed metastructure is composed of a host beam attached with alternate bistable and monostable hardening local resonators. The distributed-parameter electromechanically coupled model has been established. The dynamic mechanism of the vibration suppression performance of the proposed metastructure has been discussed. Results show that the proposed design can effectively suppress the high-amplitude resonance transmission peaks outside the bandgap and maintain a wide bandgap across a wide range of excitation levels and frequencies. In addition, a broad power bandwidth can be formed, which can be applied as a practical source of electrical energy for powering onboard microelectronic devices.

Acknowledgements. We would like to acknowledge the financial support of the Australian Research Council under Grant No. DE210101382.

References

1. Liu, Z., et al.: Locally resonant sonic materials. *Science* **289**(5485), 1734–1736 (2000)

2. Sugino, C., Xia, Y., Leadenham, S., Ruzzene, M., Erturk, A.: A general theory for bandgap estimation in locally resonant metastructures. *J. Sound Vib.* **406**, 104–123 (2017)
3. Hobeck, J.D., Inman, D.J.: Simultaneous passive broadband vibration suppression and energy harvesting with multifunctional metastructures. In: *Proceedings SPIE 10172, A Tribute Conference Honoring Daniel Inman*, p. 101720K (2017)
4. Chen, Y., Hu, G., Huang, G.: A hybrid elastic metamaterial with negative mass density and tunable bending stiffness. *J. Mech. Phys. Solids* **105**, 179–198 (2017)
5. Wang, P., Casadei, F., Shan, S., Weaver, J.C., Bertoldi, K.: Harnessing buckling to design tunable locally resonant acoustic metamaterials. *Phys. Rev. Lett.* **113**(1), 014301 (2014)
6. Nimmagadda, C., Matlack, K.H.: Thermally tunable band gaps in architected metamaterial structures. *J. Sound Vib.* **439**, 29–42 (2019)
7. Alshaqqaq, M., Erturk, A.: Graded multifunctional piezoelectric metastructures for wideband vibration attenuation and energy harvesting. *Smart Mater. Struct.* **30**(1) (2021)
8. Hu, G., Austin, A.C.M., Sorokin, V., Tang, L.: Metamaterial beam with graded local resonators for broadband vibration suppression. *Mech. Syst. Sig. Process.* **146** (2021)
9. Xiao, Y., Wen, J., Wen, X.: Broadband locally resonant beams containing multiple periodic arrays of attached resonators. *Phys. Lett. A* **376**(16), 1384–1390 (2012)
10. Mosquera-Sánchez, J.A., De Marqui, C.: Dynamics and wave propagation in nonlinear piezoelectric metastructures. *Nonlinear Dyn.* **105**(4), 2995–3023 (2021)
11. Xia, Y., Ruzzene, M., Erturk, A.: Dramatic bandwidth enhancement in nonlinear metastructures via bistable attachments. *Appl. Phys. Lett.* **114**(9) (2019)
12. Xia, Y., Ruzzene, M., Erturk, A.: Bistable attachments for wideband nonlinear vibration attenuation in a metamaterial beam. *Nonlinear Dyn.* **102**(3), 1285–1296 (2020)
13. Banerjee, A., Calius, E.P., Das, R.: An impact based mass-in-mass unit as a building block of wideband nonlinear resonating metamaterial. *Int. J. Non-Linear Mech.* **101**, 8–15 (2018)
14. Xu, C., Chen, S., Wang, C.H., Yang, Y., Zhao, L.: Amplitude-robust metastructure with combined bistable and monostable mechanisms for simultaneously enhanced vibration suppression and energy harvesting. *Appl. Phys. Lett.* **122**(15) (2023)
15. Hu, G., Tang, L., Das, R.: Internally coupled metamaterial beam for simultaneous vibration suppression and low frequency energy harvesting. *J. Appl. Phys.* **123**(5) (2018)
16. Mikoshiba, K., Manimala, J.M., Sun, C.T.: Energy harvesting using an array of multifunctional resonators. *J. Intell. Mater. Syst. Struct.* **24**(2), 168–179 (2012)
17. Bukhari, M., Barry, O.: Simultaneous energy harvesting and vibration control in a nonlinear metastructure: a spectro-spatial analysis. *J. Sound Vib.* **473** (2020)
18. Chaurha, A., Malaji, P.V., Mukhopadhyay, T.: Dual functionality of vibration attenuation and energy harvesting: effect of gradation on non-linear multi-resonator metastructures. *Eur. Phys. J. Special Top.* (2022)
19. Vasconcellos, D.P., Cruz, R.S., Fernandes, J.C.M., Silveira, M.: Vibration attenuation and energy harvesting in metastructures with nonlinear absorbers conserving mass and strain energy. *Eur. Phys. J. Spec. Top.* (2022)
20. Hu, G., Tang, L., Das, R.: Metamaterial-inspired piezoelectric system with dual functionalities: energy harvesting and vibration suppression. In: *Active and Passive Smart Structures and Integrated Systems 2017* (2017)
21. Sugino, C., Erturk, A.: Analysis of multifunctional piezoelectric metastructures for low-frequency bandgap formation and energy harvesting. *J. Phys. D Appl. Phys.* **51**(21) (2018)
22. Zhao, L.: Synchronization extension using a bistable galloping oscillator for enhanced power generation from concurrent wind and base vibration. *Appl. Phys. Lett.* **116**(5) (2020)
23. Zhao, L., Yang, Y.: Enhanced aeroelastic energy harvesting with a beam stiffener. *Smart Mater. Struct.* **24**(3) (2015)
24. Daqaq, M.F., Masana, R., Erturk, A., Dane Quinn, D.: On the role of nonlinearities in vibratory energy harvesting: a critical review and discussion. *Appl. Mech. Rev.* **66**(4) (2014)

25. Stanton, S.C., McGehee, C.C., Mann, B.P.: Nonlinear dynamics for broadband energy harvesting: investigation of a bistable piezoelectric inertial generator. *Physica D* **239**(10), 640–653 (2010)
26. Sugino, C., Leadenham, S., Ruzzene, M., Erturk, A.: On the mechanism of bandgap formation in locally resonant finite elastic metamaterials. *J. Appl. Phys.* **120**(13) (2016)